Renewable Energy 142 (2019) 137–146

Contents lists available at ScienceDirect

Renewable Energy

journal homepage: www.elsevier.com/locate/renene

Evaluation of the near future wave energy resources in the Black Sea under two climate scenarios

Liliana Rusu

Department of Mechanical Engineering, Faculty of Engineering, 'Dunarea de Jos' University of Galati, 111 Domneasca St., 800 201, Galati, Romania

ARTICLE INFO

Article history:
Received 23 November 2018
Received in revised form
14 April 2019
Accepted 18 April 2019
Available online 23 April 2019

Keywords:
Climate change
Wave power
SWAN
Black Sea
Near future projection

ABSTRACT

The objective of this study is to evaluate the near future wave power resources (2021–2050) in the Black Sea, based on the results coming from a wave modelling system forced with wind fields provided by a Regional Climate Model (RCM). Such wind fields have been produced in the framework of the EURO-CORDEX experiment. They cover the entire European domain and have a resolution of 0.11°. Two different wind fields are considered in the wave model simulations, according to two Representative Concentration Pathways (RCPs) scenarios, namely RCP4.5 and RCP8.5. The SWAN (Simulating Waves Nearshore) model, which has been implemented over entire the Black Sea basin, is considered for the wave energy predictions. Furthermore, in order to estimate the impact of climate change on the wave energy resources in the Black Sea basin, the results obtained in the near future 30-year period (covering the early 21st century) are compared with historical data. These are the wave energy resources resulted from SWAN model simulations performed also for a 30-year (1976–2005) time-slice. Thus, these historical wave energy resources are obtained using historical RCM wind fields to force the wave model. The results show an increase in the range 0.05–0.18 kW/m (a rise of 5–16%) of the mean wave power under RCP4.5 scenario in almost all the western part of the Black Sea and also in the north-eastern area, while under RCP8.5 is quite double in. On the other hand, the linear regressions fitted to the annual means computed to each 30-year time-slice in 8 reference points did not indicate significant trends.

© 2019 Elsevier Ltd. All rights reserved.

1. Introduction

The increasing investments in renewable energy require also an estimation of the future evolution of these resources. On the other hand, in the last years, a higher dynamics of the environmental parameters can be noticed in the Black Sea [1], and also in other areas or as the west Iberian coast [2] or the Mediterranean Sea [3]. This leads very often to substantial reconfigurations of the environmental matrix. Furthermore, as regards the marine and coastal environments such reconfigurations of the environmental matrix are even stronger and can lead to extreme events that may affect both navigation as well as the human activities taking place in the nearshore [4]. From this perspective, climate change also represents a challenge for the ocean energy sector, where the renewable energy extracted from waves and wind has an important role [5].

Wave energy is abundant since there are large spaces in the nearshore having a great potential, which expects to be exploited. However, an assessment of the available resources is necessary and this issue have been the topic of several recent studies, from the global scale [6], to regional domains such Puerto Rico and the United States (US) Virgin Islands [7], US Gulf of Mexico [8], south of the Brazilian coast [9], Peru [10], Azores islands [11], Portuguese continental coast [12], Caribbean area [13], French coast [14], Mediterranean Sea [15], Greek offshore areas [16], Australia [17] and China adjacent seas [18]. Such studies are very useful for wave farm planning [19,20]. It might be also important to mention that wave energy has a higher density than solar or wind energy as well as a higher predictability [21].

Nowadays there are various Wave Energy Converters (WECs) that have different wave power matrices and for this reason their performance depends on the wave characteristics in the location where they are deployed. The performance of some state-of-the-art wave energy converters was evaluated in locations with the worldwide highest wave power [22], and also along the European continental coasts [23]. In addition, the seasonal and inter-annual variations could also significantly influence the performance of the WEC systems and this variability needs to be studied [24]. An

E-mail address: lrusu@ugal.ro.

https://doi.org/10.1016/j.renene.2019.04.092
0960-1481/© 2019 Elsevier Ltd. All rights reserved.

optimum hotspot identifier was developed by Kamranzad et al. [25] that takes into account the mean wave power, the frequency of wave power greater than a threshold and the monthly variability. New types of WECs are designed and tested targeting lower Levelized Cost of Energy (LCoE) [26] or improved versions of devices are developed [27].

Another relevant aspect is related to the fact that the future marine energy farms, by extracting the wave power, may become also a significant player in the coastal protection [28,29,30]. This is because usually the nearshore areas rich in wave energy are also subjected to significant coastal processes that may affect very much the shoreline dynamics. Thus, the extraction of the wave power obviously diminishes the amount of energy which is dissipated in the surf zone attenuating the intensity of the coastal processes. Recent studies, based on the observations in field campaign [31] or basin experiments [32], evaluate the ability of the numerical models to simulate the modification of the wave characteristics due to the presence of the WECs.

Furthermore, another important issue is related to the very high dynamics in the development of offshore wind exploitation. Nowadays, the price of the energy extracted from the offshore wind makes it economically efficient and moreover in the very near future this is expected to become about half of the price of the atomic power. It means that an explosion of the offshore wind industry is expected in the next years and this will influence also in a positive way the development of the wave energy conversion technologies since the wave farms could use the infrastructure of the wind farms by the collocation process, or by developing hybrid wind-wave farms [33]. In such a case, the wave farm can provide protection to the wind farm and the entire farm can provide coastal protection [34,35,36]. This means that there are a lot of premises to assume that wave energy will become an important player in the global energy portfolio.

The target area of the present work is the Black Sea. This is an enclosed sea basin that can be seen also as the most distant extension of the North Atlantic Ocean, to which is linked via the Mediterranean Sea. Various studies concerning the wave climate in the Black Sea have been already performed [37,38,39]. Data assimilation methods were also used to improve the wave model results at a local scale [40,41], or over the entire basin [42,43]. The evaluation of the wave energy in the Black Sea represented the target of other studies [44,45]. The variability of the wave energy was also highlighted [46,47]. In the above mentioned references, the wave energy was evaluated for shorter periods than 30-year, or in the case of longer periods (as [47]) less reliable data were used to assess the wave energy, namely visual wave observations. Most of these studies show that the wave conditions in the Black Sea are very sensitive to climate changes, especially as regards the changes of the wind fields. Thus, the changes expected in the configuration of the environmental matrix may also induce new and completely different patterns in the future wave climate, modifying also the wave power spatial distribution in the geographical space of the Black Sea, as well as the locations of the hot spots. These are marine areas where the wave power is considerably higher in relationship with the neighbouring places.

From this perspective, the main objective of the present work is to provide relevant information concerning future wave energy patterns in the basin of the Black Sea. This implies the 30-year time interval (2021–2050). For this, a wave modelling system based on the SWAN model (acronym from Simulating Waves Nearshore, [48,49]), has been used. The model is based on the spectrum concept and the main forcing factor is represented by the wind fields. Thus, the wind fields provided by a Regional Climate Model (RCM) have been considered for forcing the SWAN model. Two wind fields are considered in the wave model simulations, according to two Representative Concentration Pathways (RCPs) emission scenarios [50], namely RCP4.5 and RCP8.5. Furthermore, in order to estimate the impact of climate changes on the wave energy resources in the Black Sea basin, the results obtained in the near future 30-year period (covering the time interval 2021–2050) were compared with the historical conditions simulated also for a 30-year time interval (1976–2005) and considering the historical RCM wind fields to force the wave model. At this point it has to be also highlighted that such studies providing projections in terms of the wave power, as resulted from the simulations carried out by a spectral wave model forced by RCM wind fields under various RCP scenarios were not yet conducted.

2. Methods and materials

The spectral phase-averaged wave models resolve an advection type equation that gives the propagation of the wave spectrum in a space defined by five dimensions. These are time, the geographical spaces defined by two dimensions which in spherical coordinates are the latitude and longitude and the spectral space defined by the relative frequency (σ) and the mean wave direction (θ) [51,52]:

$$\frac{DN}{Dt} = \frac{S}{\sigma} \tag{1}$$

The spectrum considered is the action density spectrum (N), rather than the energy density spectrum, because in the presence of the currents, action density is conserved while energy density is not. This is, in fact, the energy density (E) divided by the relative frequency. S from the right-hand side of equation (1) represents the source terms. As regards the deep water processes, three components are more relevant. These correspond to the wind input (S_{in}), nonlinear wave-wave interactions (S_{nlq}) of quadruplet type and whitecapping dissipation (S_{disw}). Besides, such processes, in intermediate and shallow water some other source terms become relevant. They correspond to phenomena as bottom friction (S_{bf}), depth-induced wave breaking (S_{br}) or triad nonlinear wave-wave interactions (S_{tr}) and have very often important roles. In consequence, the total source becomes:

$$S = S_{in} + S_{nlq} + S_{disw} + S_{bf} + S_{br} + S_{tr} + \ldots. \tag{2}$$

For large geographical spaces considered for model simulations, the governing equation (1) is expressed in spherical coordinates, longitude (λ) and latitude (φ):

$$\frac{\partial N}{\partial t} + \frac{\partial}{\partial \lambda}\dot{\lambda}N + \frac{1}{\cos\varphi}\frac{\partial}{\partial \varphi}\dot{\varphi}N\cos\varphi + \frac{\partial}{\partial \sigma}\dot{\sigma}N + \frac{\partial}{\partial \theta}\dot{\theta}N = \frac{S}{\sigma} \tag{3}$$

In the wave models based on the spectrum concept, the components of the energy transport per unit length of the wave front, expressed in W/m, denoted also as wave power, are computed with the relationships [53]:

$$\begin{aligned} Etr_x &= \rho g \iint c_x E(\sigma,\theta) d\sigma d\theta \\ Etr_y &= \rho g \iint c_y E(\sigma,\theta) d\sigma d\theta \end{aligned} \tag{4}$$

In the above equation, x, y are the problem coordinate system (for the spherical coordinates x-axis corresponds to longitude and y-axis to latitude), $E(\sigma,\theta)$ the wave energy spectrum and c_x, c_y are the propagation velocities of wave energy in the geographical space (absolute group velocity components) defined as:

$$c_x = \dot{x},\ c_y = \dot{y}, \tag{5}$$

Finally, the absolute value of the wave power in each point of the computational grid is:

$$Etr = \sqrt{Etr_x^2 + Etr_y^2} \quad (6)$$

A wave modelling system, SWAN based, has been implemented in the basin of the Black Sea and extended validated against both in situ and remotely sensed measurements [54,55]. So, it results can be considered accurate and reliable. The computational grid (structured grid) coincides with the bathymetric grid and has 176 points in the x-direction and 76 points in the y-direction. The resolution in the geographical space is 0.08° × 0.08° and in the spectral space 30 × 36 (30 frequencies logarithmically spaced from 0.05 to 1.0 Hz and 36 directions). The computational domain of the SWAN model implementation is illustrated in Fig. 1. In each point of the SWAN computational domain information about the main wave parameters are delivered with 3-h time resolution.

Besides the wind forcing, all the other relevant physical processes (whitecapping, quadruplet and triad wave-wave interactions, bottom friction, wave breaking, etc.) have been considered. Table 1 presents additional details about the physical parameterizations and the input considered in the SWAN (version 40.91ABC) simulations. Moreover, the computational strategies developed together with the experience acquired by the implementation of similar wave modelling systems based on the SWAN model implemented in other marine environments have been also considered [57,58]. As a result, the wave prediction provided by the modelling system implemented in the basin of the Black Sea can be considered in general reliable. The most important factor for a good prediction of the wave fields is represented by the accuracy and resolution of the wind fields considered for model forcing.

The Intergovernmental Panel on Climate Change (IPCC) experts, in collaboration with the climate modelling community, selected four Representative Concentration Pathways (RCPs). These RCPs are based on some prescribed pathways for greenhouse gas (GHG) and other forcing agents, and they cover the plausible global warming scenarios [50,59]. The four RPCs are named according to the radiative forcing expected to be produced by the end of the 21st century and together span the range of radiative forcing values from 2.6 to 8.5 W/m2 (RCP2.6, RCP4.5, RCP6.0 and RCP8.5). The Global Climate Models (GCMs) are used for generating global climate change projections. These models also provide the boundary conditions for the Regional Climate Models (RCMs). Under each scenario, the climate models predict the future values of various variables, one of them being the wind speed (zonal and meridional components of wind velocity).

The wind fields used to force the SWAN model are those carried out by SMHI (Swedish Meteorological and Hydrologic Institute) with a RCM, namely the Rossby Centre regional atmospheric model (version RCA4) [60], in the framework of the EURO-CORDEX experiment. These wind fields cover the entire European domain, including also the basin of the Black Sea [61,62]. A detailed analysis of these winds over the Black Sea basin was made by Ref. [63]. The boundary conditions provided by EC-EARTH, operated by the Irish Centre for High-End Computing (ICHEC-EC-EARTH), were considered to force the RCA4 model.

In order to assess the impact of the climate changes on the near future wave energy resources in the Black Sea Basin, three types of wind fields are used for wave model simulations. The first two wind fields were simulated under RCP4.5 and RCP8.5 emission scenarios and cover a 30-year period (2021–2050) representing the near future. The first scenario considers moderate future greenhouse gas concentration scenario and the stabilization of radiative forcing to 4.5 W/m^2 (~650 ppm atmospheric CO2 equivalent) at the end of the 21st century, while for the second a rising radiative forcing pathway leading to 8.5 W/m^2 (>1370 ppm atmospheric CO2 equivalent) by 2100 is counted. The third set represents historical simulations of the wind fields that cover also a 30-year time interval (1976–2005). The CMIP5 historical simulations use the observed historical forcing conditions such as observed greenhouse gas and aerosol concentrations [64]. All wind fields are provided at 10 m height and the spatial and temporal resolution are 0.11° (EUR-11, ~12.5 km) and 6-h, respectively.

3. Results and discussions

The spatial distributions of the wave power corresponding to the near future (2021–2050) are computed based on the energy transport output of the SWAN model, forced with wind fields simulated under the climate projections made by RCP4.5 and RCP8.5 scenarios. The wave power in each grid point of the computational domain covering the Black Sea basin is provided with a temporal resolution of 3 h. Then, the time series of wave power are averaged and the spatial distribution of mean wave power is computed based on these data. The mean wave power fields for RCP4.5 and RCP8.5 scenarios are represented in Fig. 2 and both show a maximum value of 3.8 kW/m, whose geographic position is indicated by a white circle. The mean direction of the energy transport, computed by averaging separately its components in the geographical space, is also represented with white arrows

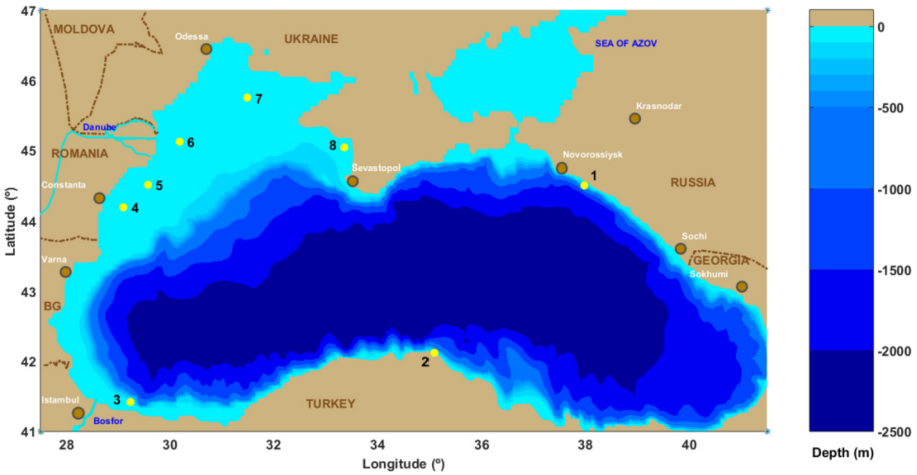

Fig. 1. The bathymetry of the Black Sea and the locations of 8 reference points selected for local analysis.

Table 1
Physics and input considered in the SWAN simulations.

Input and process	Grid
Bathymetry	General Bathymetric Chart of the Oceans (GEBCO)
Wind forcing	Wind fields at 10 m over sea level from EURO-CORDEX databases
Computational mode	Non-stationary
Time step	10 min
Numerical scheme	Second-order upwind scheme (default)
Bottom friction	Activated (default option)
Quadruplet nonlinear interactions	Activated (default option)
Exponential growth by wind	Janssen formulation [56]
Whitecapping	Activated, Janssen formulation [56]
Breaking	Activated (default option)

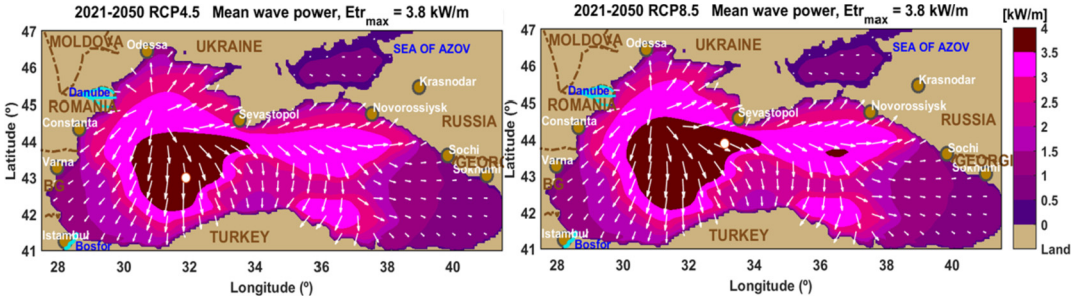

Fig. 2. The spatial distribution of the mean wave power fields and the mean direction of the energy transport corresponding to the near future (2021–2050) for two emission scenarios: RCP4.5 (left) and RCP8.5 (right).

scaled with the wave power background field. No significant differences between the patterns of two mean wave power fields are observed.

In order to evaluate the possible effects of the climate change projections on the wave power in the Black Sea basin, another set of SWAN simulations was performed using historical wind fields to force the wave model. The wave power field obtained by averaging 30-year SWAN model results (1976–2005) is presented in Fig. 3. Besides a slight drop of the maximum wave energy (0.1 kW/m), no significant alterations are observed in the pattern of the wave power fields.

The assessment of the projected changes in terms of mean wave power was made by calculating the difference between the results obtained for RCP4.5 and RCP8.5 scenarios, respectively, and those corresponding to the historical runs. The differences between the mean wave powers, projected and historical values, were calculated in each point of the computational domain. After this, the maps of the spatial distribution of these differences have been designed. These results are presented in Fig. 4. In the case of RCP4.5 scenario, higher mean values of the wave power with about 0.05–0.18 kW/m (an increase ranging between 5 and 16%) than those simulated for the historical period are encountered in the western part of the Black Sea basin and also in the north-eastern area. In the south-western part of the basin (in front of the Turkish coast) the maximum difference about 0.18 kW/m can be found. On the other hand, a decrease of the average wave power with about 0.1 kW/h (around 9%) is observed in the south-eastern side of the basin.

As regards the mean values of the wave power obtained under the RCP8.5 scenario, the comparison with the historical data shows

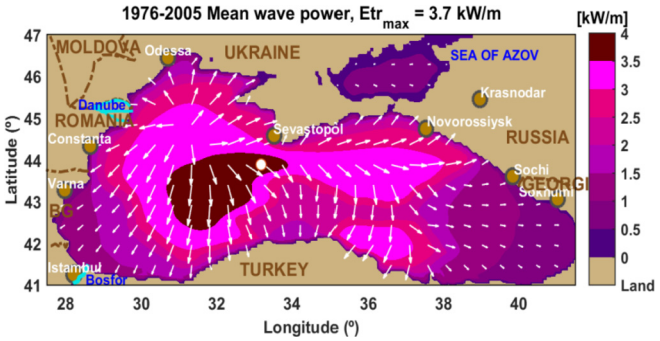

Fig. 3. The spatial distribution of the mean wave power fields and the mean direction of the energy transport corresponding to the 30 year period 1976–2005.

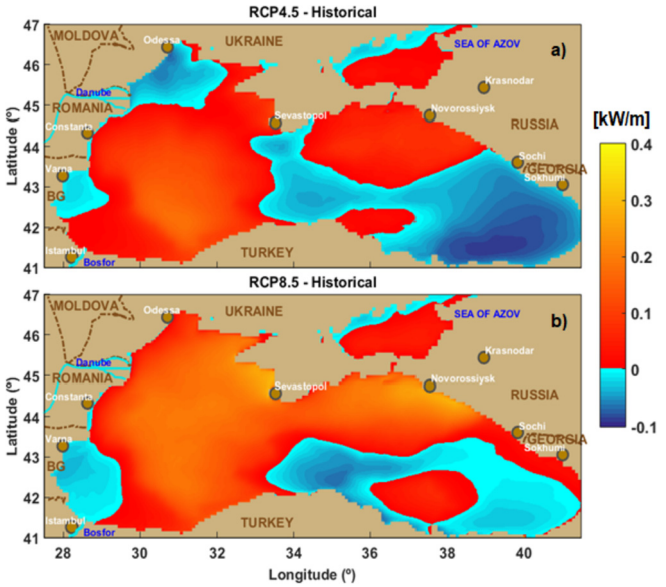

Fig. 4. Differences between the mean wave power for (a) RCP4.5 scenario, (b) RCP8.5 scenario and historical runs.

a higher increase (almost double) than in the case of RCP4.5 in the same regions (even a little bit extended). The locations with the highest increase by up to 0.4 kW/m (representing a rise of about 22%) are near Novorossiysk (Russian coast) and Sevastopol (Ukrainian coast). Only in few regions in south and south-east a small decrease by about 0.07 kW/m is observed.

Previous studies indicated the existence of a strong seasonal variability of the wave power [45,47,65]. Projections of the mean wave power fields, corresponding to the near future for each season, under both RCP 4.5 and RCP 8.5 scenarios, are shown in Fig. 5, while the historical means are illustrated in Fig. 6. The following seasonal partition was considered to compute the average values: winter - DJF (December-January-February), spring - MAM (March-April-May), summer - JJA (June-July-August) and autumn - SON (September-October-November).

An overall analysis of the mean wave power fields along the annual seasons shows that both projections maintain the same pattern for the near future as those from the historical simulations. Comparing now the results obtained in each season, it can be observed that the wave power projections for autumn are quite equal, with a maximum value of around 4.1 kW/m and a similar geographical position. Looking now at the historical means, the same pattern of the mean wave power can be seen, but with a smaller maximum value (3.9 kW/m).

In the winter time, the mean wave power for RCP4.5 is just a little less than for RCP8.5 (about 0.3 kW/m), but both are higher than the historical means. The highest differences between mean wave power fields are observed in the springtime. The means computed from the historical simulations are in the middle (maximum value is 3.5 kW/m), while the RCP8.5 projection showing higher values (maximum 3.7 kW/m) and RCP4.5 with lower values of the mean wave power (3.3 kW/m). In the summertime, the wave power fields are higher for the historical data (about 0.2 kW/m) than in the projections corresponding to the near future.

As in the case of the analysis regarding the evolution of the mean wave power over the entire 30-year period corresponding to the near future, the assessment of the expected changes in terms of

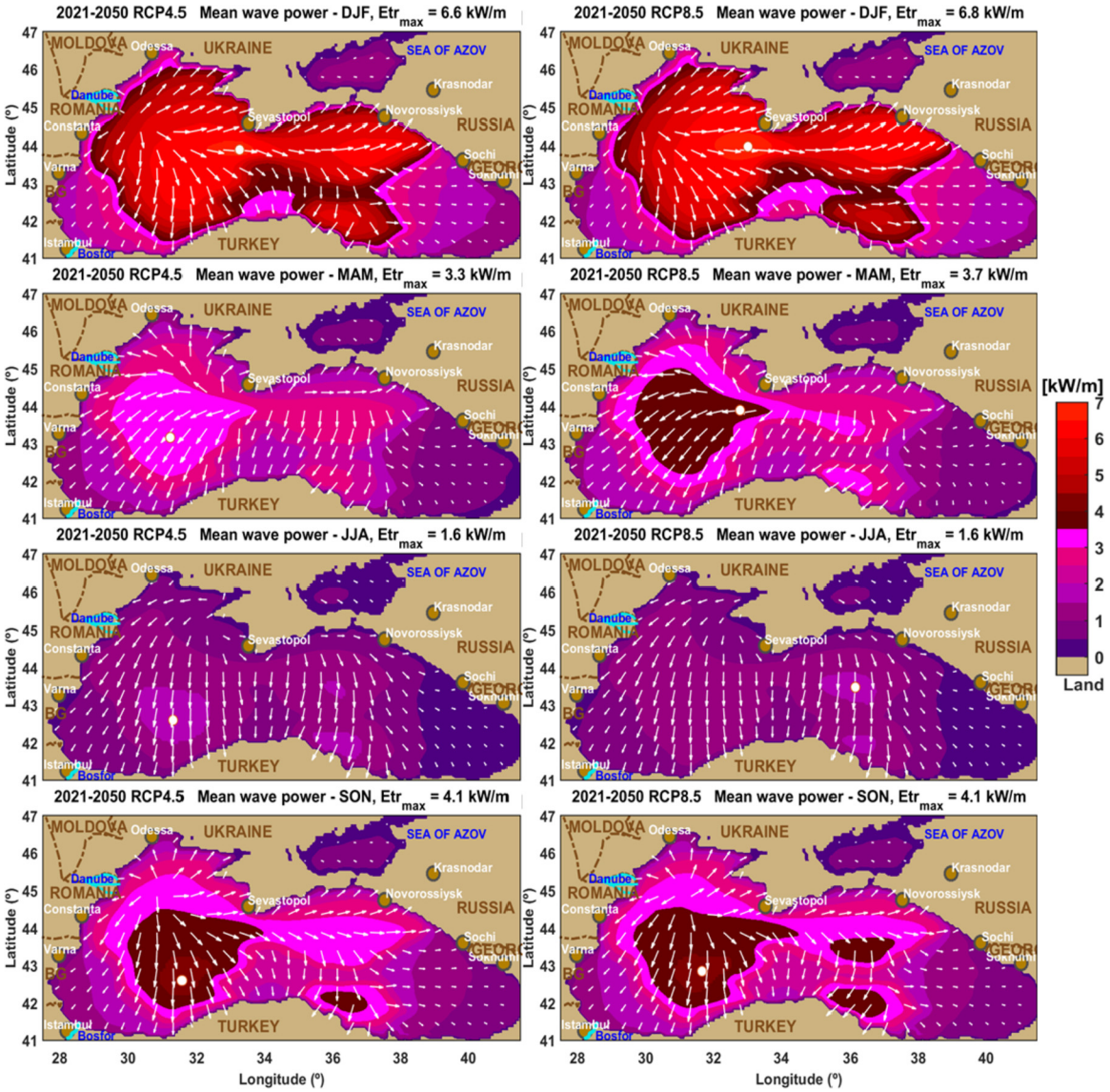
2021-2050 RCP4.5 Mean wave power - DJF, Etr max = 6.6 kW/m
2021-2050 RCP8.5 Mean wave power - DJF, Etr max = 6.8 kW/m
2021-2050 RCP4.5 Mean wave power - MAM, Etr max = 3.3 kW/m
2021-2050 RCP8.5 Mean wave power - MAM, Etr max = 3.7 kW/m
2021-2050 RCP4.5 Mean wave power - JJA, Etr max = 1.6 kW/m
2021-2050 RCP8.5 Mean wave power - JJA, Etr max = 1.6 kW/m
2021-2050 RCP4.5 Mean wave power - SON, Etr max = 4.1 kW/m
2021-2050 RCP8.5 Mean wave power - SON, Etr max = 4.1 kW/m
MOLDOVA
UKRAINE
SEA OF AZOV
ROMANIA
RUSSIA
TURKEY
Odessa
Krasnodar
Sevastopol
Novorossiysk
Sochi
Constanta
Varna
Istambul
Bosfor
Danube
Latitude (°)
Longitude (°)
[kW/m]
Land

Fig. 5. Seasonal variation of the mean wave power fields and the mean direction of the energy transport corresponding to the 30-year near future (2021–2050) for two emission scenarios: RCP4.5 (left) and RCP8.5 (right). From top to bottom: DJF, MAM, JJA and SON.

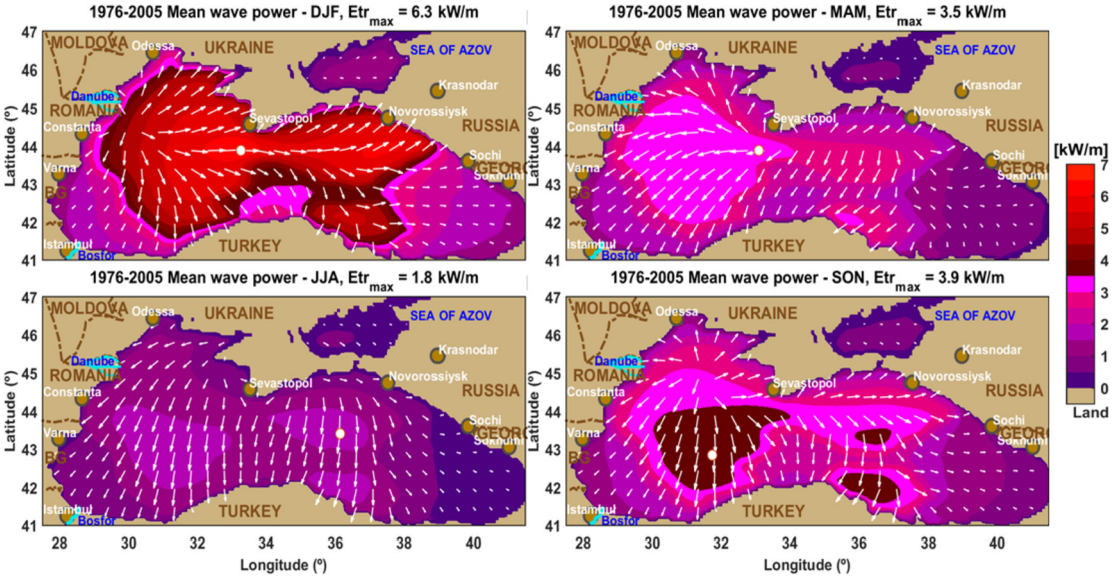

Fig. 6. Seasonal variation of the mean wave power fields and the mean direction of the energy transport corresponding to the 30-year period 1976–2005. From left to right: MAM, JJA, SON and DJF.

the mean wave power is now analyzed for each season and scenario, respectively. The spatial distribution of the seasonal differences between the results obtained for RCP4.5 and RCP8.5 scenarios and those corresponding to the historical runs are presented in Fig. 7.

Under RCP4.5 scenario, the mean wave power in the winter season (DJF) is projected to increase by up to 0.92 kW/m (an increase ranging between 10 and 32%) in the central zone of the western area (the Romanian nearshore and close to the Turkish coast), while in the south-eastern area a decrease of about 0.17 kW/m is expected (about 12%). In the case of the RCP8.5 scenario, the areas with the highest increase are the same as those previously

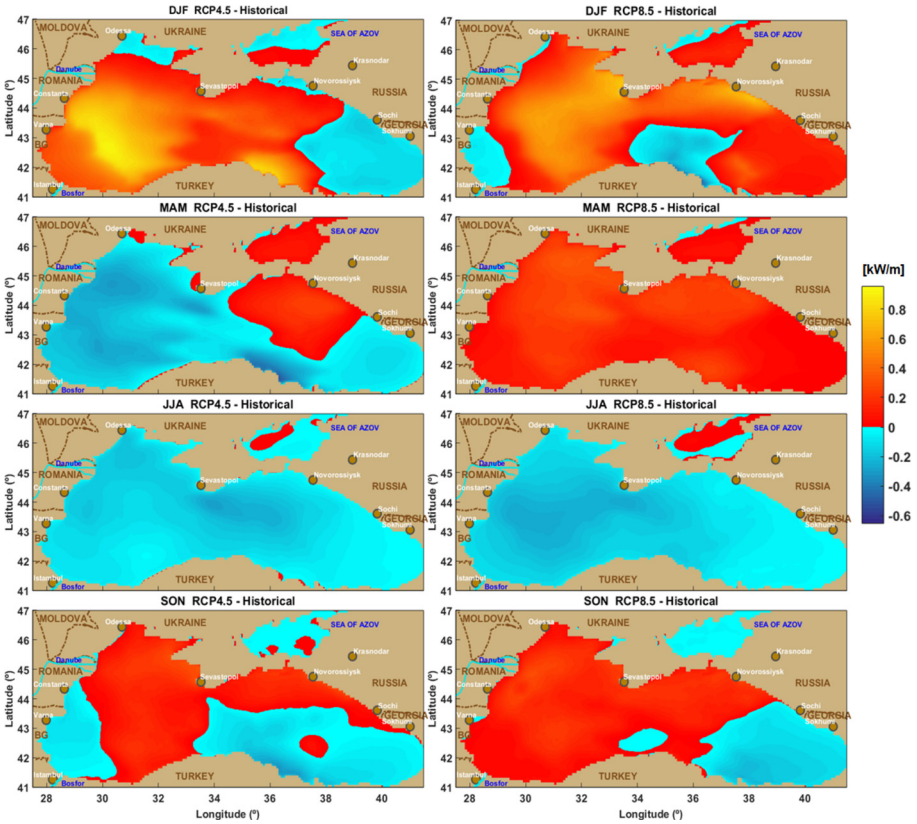

Fig. 7. Seasonal differences between the mean wave power for the two emission scenarios: RCP4.5 (left) and RCP8.5 (right) and the historical runs. From the top to the bottom: DJF, MAM, JJA and SON.

pointed out for the entire 30-year period (see Fig. 4b), but the increase is more accentuated (by almost 0.8 kW/m, a rise up to 27%). Only in some small areas the projected values of the mean wave power show a decrease, namely in the south-west (in front of Bulgarian coast) about 0.2 kW/m (a decrease by 8%) and in the central area of the Turkish coast about 0.45 kW/m (representing a decrease of 26%).

The projected changes in the spring season (MAM) have different behaviour for the two scenarios. Thus, in almost the basin of the Black Sea a decrease of the mean wave power resulted from the projections under the RCP4.5 scenario is expected (with a maximum change in the central area of the Turkish coast of about 0.62 kW/m), while under RCP8.5 over the entire basin an increase ranging between 0.2 and 0.4 kW/m is expected. In summer (JJA) under both scenarios a decrease of the mean wave power is expected (around 0.3 kW/m), and only in the Azov Sea the same mean values as in the historical period will be maintained. In autumn (SON) the greatest increase of the mean wave power is projected on the western side of the Black Sea basin (0.35–0.4 kW/m) for both scenarios (except the south-western area under RCP4.5 when a decrease is expected). In the south-eastern area a decrease ranging from 0.2 to 0.3 kW/m is noticed.

For a local analysis of the wave power characteristics eight reference points (see Fig. 1) were chosen along the coastal areas of the Black Sea. The geographical coordinates of these points are indicated in Table 2, together with the corresponding water depth, which is important for wave energy farms implementation. In general, the point locations were selected in areas showing higher average wave power values and water depths ranging between 30 and 80 m (except P1).

The points P1 and P2 are in the eastern part of the Black Sea, while the other six points are located in the western part. The first eastern point is near to Gelendzhik city, located in the southeast of an important Russian port (Novorossiysk), while the second is close to Cape Sinope, the most northern edge of the Turkish side of the Black Sea coast. The third point is located in the offshore of Istanbul, followed by three points that cover the offshore area of the Romanian coast. Finally, the last two points are near the Ukrainian coast. Some statistical parameters as mean and maximum values, skewness index (Skew), standard deviation (Std) and 95th percentile were computed in each reference point and the results are presented in Table 1 and Fig. 8.

As regards the 95th percentile, the lowest values (around 6 kW/m) are found in the southern points (P2 and P3) while in all other points the percentile values are higher than 10 kW/m. No significant difference can be observed between the results from various simulations. The standard deviations have the same pattern as the 95th percentiles, with the mention that the results for the RCP8.5 scenario show the highest values while the lowest values

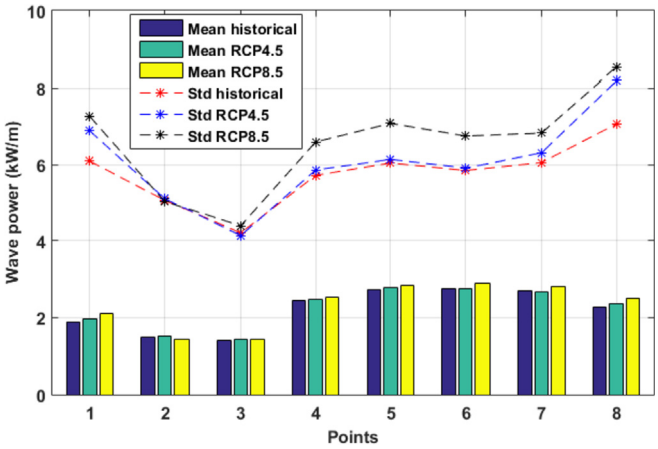

Fig. 8. Mean values and standard deviations of the wave power computed in each reference point for each 30-year time interval considered.

correspond to the historical simulations. Mean values higher than 2 kW/m are noticed in the points P4÷P8, in all these points the mean wave powers for RCP8.5 scenarios are the highest. In the western points (P4÷P6) the lowest values of the skewness indexes were computed, with values ranging from 6 to 7 for historical and RCP4.5 simulations, and from 8 to 9 for the RCP8.5 results. In P2, the skewness index is about 10 for all simulations, while P1 and P8 show similar patterns – the highest values correspond for RCP8.5, followed by RCP4.5 and the lowest are in the historical simulations. As regards the maximum values, P8 presents the highest values for all simulations.

The next step in the local analysis is to evaluate the inter-annual variability and possible trends of the wave power during every 30-year period of simulations. For each reference point annual mean values of the wave power were computed for historical simulations, and also for RCP 4.5 and RCP 8.5 scenarios. The annual means obtained only for P1 (an eastern point) and P5 (a western point) are presented as bars in Fig. 9. In all cases an inter-annual variability of the wave power was observed.

In order to highlight some possible trends of the annual data, a five-year running average was applied to filter the data variability (solid lines denoted with MA in Fig. 9). For each case a linear trend was also fitted and represented by dashed lines (denoted LT) in Fig. 9. The slope of the linear regression adjusted to the annual means for historical simulations shows in P1 a slight decrease of the annual means with about 4 W/m per decade while in P5 is about 140 W/m per decade. Only in the points P2 an increase in the annual mean was calculated (see Table 3).

The annual means computed for RCP 4.5 scenario show an

Table 2
Wave power characteristics corresponding to the reference points computed for each 30-year time interval considered.

Points		P1	P2	P3	P4	P5	P6	P7	P8
Longitude (°)		37.98	35.09	29.23	29.1	29.56	30.18	31.49	33.36
Latitude (°)		44.51	42.12	41.42	44.2	44.52	45.12	45.75	45.04
Depth (m)		198	61	77	41	47	33	38	69
Historical	Max (kW/m)	201.7	146.5	185.7	188.8	174.9	142.8	164.3	273.8
	Skew	9.15	9.31	13.53	7.97	7.05	6.07	6.10	8.94
	95^{th} (kW/m)	9.33	7.11	6.07	10.37	11.59	11.88	12.07	10.76
RCP4.5	Max (kW/m)	331.8	161.4	203.5	151.1	135.3	156.2	254.2	461.9
	Skew	14.23	9.27	11.39	7.38	6.56	6.24	8.47	15.39
	95^{th} (kW/m)	9.55	7.10	6.25	10.43	11.68	11.87	11.87	11.06
RCP8.5	Max (kW/m)	307.3	151.9	129.3	189.8	272.0	219.1	175.8	360.7
	Skew	11.15	9.99	10.54	9.21	8.89	7.76	7.15	11.87
	95^{th} (kW/m)	10.09	6.46	5.84	10.14	11.55	12.03	12.65	11.65

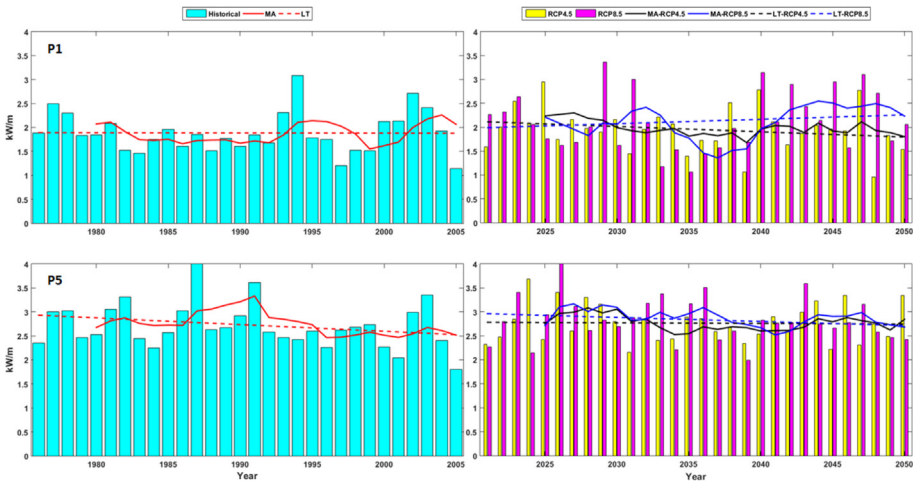

Fig. 9. Annual mean (bars), five-year running average (MA) and linear trend (LT) of the wave power computed in two reference points for the historical simulations (left) and for both emission scenarios (right).

Table 3
Linear trends of the annual means of wave power, in W/m per decade.

Simulations	Points							
	P1	P2	P3	P4	P5	P6	P7	P8
Historical	−4	6	−168	−121	−140	−149	−164	−55
RCP4.5	−109	87	41	−13	−13	−21	−42	−95
RCP8.5	92	−29	−25	−103	−85	−6	105	89

upward trend in the points P2 and P3 while in all other points a downward trend was observed. In the case of RCP 8.5 scenario an upward trend exists only in three points (P1, P7 and P8). Analyzing now all the points and the consistency of the linear trends along the historical and near future simulations, it can be observed that in the points P3÷P6 the same descending trend is maintained, but with a reduced slope compared with the historical results.

The five-year running average lines for points located in front of the Romanian coast (P4, P5 and P6), and also P3, show that light variations along the 30-year period for both scenarios were observed (similar with those P5 illustrated in Fig. 9). In all other points the variability pattern of the five-year running average lines follows the one encountered in P1, especially as regards the mean wave power simulated for the RCP 8.5 scenario. In this case a decrease of the annual means can be observed in the interval 2035–2040, followed by a sharp rise.

4. Conclusions

The aim of the present study was to evaluate the effect of climate change over the dynamics of the wave power in the Black Sea. High-resolution simulations with the SWAN model were carried out for two 30-year periods, when the wave model was forced with various RCM wind fields. The wave power derived for the first period (1976–2005) represents the historical conditions, while those computed for the second period (2021–2050), for two emission scenarios RCP4.5 and RCP8.5, represent projections of the future conditions.

In the case of RCP4.5 scenario, the mean wave power in the western part of the Black Sea basin shows an increase of about 0.05–0.18 kW/m, representing a rise ranging between 5 and 16% compared with the historical period. In the north-eastern area of the basin the same behaviour can also be noticed. On the other hand, the south-eastern side of the basin is affected by a decrease in the average wave power with about 0.1 kW/h (around 9%).

From the comparison of the mean wave power under the RCP8.5 scenario with the historical data a higher increase (almost double) than in the case of RCP4.5 is observed in the same regions. The highest differences about 0.4 kW/m (representing a rise of about 22%) are near Novorossiysk (Russian coast) and Sevastopol (Ukrainian coast). A small decrease by about 0.07 kW/m is observed in the south and south-eastern areas. The results obtained are in line with those reported by Mentaschi et al. [66] for the Black Sea coastal area, based on global data with lower resolution.

The seasonality of the mean wave power observed in the historical simulations is also maintained in both future projections, even with a more accentuated difference between winter and summer conditions. A local analysis of the wave power characteristics was also carried out in eight reference points located along the coastal areas of the Black Sea. The annual means were computed for each period and a linear regression was adjusted to the data. No significant trends were found.

Acknowledgment

This work was supported by a grant of Romanian Ministry of Research and Innovation, CNCS-UEFISCDI (the Romanian Funding Agency forScientific Research), project number PN-III-P4-ID-PCE-2016-0028 (Assessment of the Climate Change effects on the WAve conditions in the Black Sea – ACCWA), within PNCDI III (the Romanian National Program for Research,Development and Innovation).The wind fields used in this study have been obtained from the EURO-CORDEX data servers.

The authors would like also to express their gratitude to the reviewers for their constructive suggestions and observations that helped in improving the present work.

Nomenclature

CMIP5	Climate Model Intercomparison Project phase 5
CORDEX	Coordinated Regional Climate Downscaling Experiment
E	energy density
*E*tr	energy transport (wave power) per unit length of wave front, expressed in W/m
GCM	Global Climate Model
GHG	greenhouse gas
IPCC	Intergovernmental Panel on Climate Change

LCoE	Levelized Cost of Energy
LT	linear trend
MA	five-year running average
Max	Maximum value
Mean	Mean value
N	action density spectrum
ppm	parts per million
RCA4	Rossby Centre regional atmospheric model, version 4
RCM	Regional Climate Model
RCP	Representative Concentration Pathway
S	source term in SWAN model
Skew	Skewness
SMHI	Swedish Meteorological and Hydrologic Institute
Std	Standard deviation
SWAN	Simulating WAves Nearshore
WECs	Wave Energy Converters
95^{th}	95 percentile
λ	longitude
φ	latitude
σ	relative frequency
θ	mean wave direction

References

[1] E. Rusu, An analysis of the storm dynamics in the Black Sea, Ro. J. Techn. Sci. Appl. Mech. 63 (No. 2) (2018) 127–142.
[2] M. Bernardino, C. Guedes Soares, Evaluating Marine Climate Change in the Portuguese Coast during the 20th Century, Maritime transportation and harvesting of sea resources – Guedes Soares & Teixeira, 2018, pp. 1089–1095.
[3] C. Makris, P. Galiatsatou, K. Tolika, C. Anagnostopoulou, K. Kombiadou, P. Prinos, K. Velikou, Z. Kapelonis, E. Tragou, Y. Androulidakis, et al., Climate change effects on the marine characteristics of the Aegean and Ionian Seas, Ocean Dynam. 66 (No. 12) (2016) 1603–1635.
[4] L. Rusu, D. Butunoiu, E. Rusu, Analysis of the extreme storm events in the Black Sea considering the results of a ten-year wave hindcast, J. Environ. Protect. Ecol. 15 (No. 2) (2014) 445–454.
[5] D. Ganea, V. Amortila, E. Mereuta, E. Rusu, A joint evaluation of the wind and wave energy resources close to the Greek islands, Sustainability 9 (No. 6) (2017) 1025.
[6] B.G. Reguero, I.J. Losada, F.J. Méndez, A global wave power resource and its seasonal, interannual and long-term variability, Appl. Energy 148 (2015) 366–380.
[7] M.F.C. Silander, C.G.G. Moreno, On the spatial distribution of the wave energy resource in Puerto Rico and the United States Virgin Islands, Renew. Energy 136 (2019) 442–451.
[8] F. Haces-Fernandez, H. Li, D. Ramirez, Wave energy characterization and assessment in the US Gulf of Mexico, east and west coasts with energy event concept, Renew. Energy 123 (2018) 312–322.
[9] R.C. Lisboa, P.R. Teixeira, C.J. Fortes, Numerical evaluation of wave energy potential in the south of Brazil, Energy 121 (2017) 176–184.
[10] M. López, M. Veigas, G. Iglesias, On the wave energy resource of Peru, Energy Convers. Manag. 90 (2015) 34–40.
[11] L. Rusu, C. Guedes Soares, Wave energy assessments in the Azores islands, Renew. Energy 45 (2012) 183–196.
[12] D. Silva, E. Rusu, C. Guedes Soares, High-resolution wave energy assessment in shallow water accounting for tides, Energies 9 (No. 9) (2016) 761.
[13] C.M. Appendini, C.P. Urbano-Latorre, B. Figueroa, C.J. Dagua-Paz, A. Torres-Freyermuth, P. Salles, Wave energy potential assessment in the Caribbean Low Level Jet using wave hindcast information, Appl. Energy 137 (2015) 375–384.
[14] M. Gonçalves, P. Martinho, C. Guedes Soares, A 33-year hindcast on wave energy assessment in the western French coast, Energy 165 (2018) 790–801.
[15] G. Besio, L. Mentaschi, A. Mazzino, Wave energy resource assessment in the Mediterranean Sea on the basis of a 35-year hindcast, Energy 94 (2016) 50–63.
[16] G. Emmanouil, G. Galanis, C. Kalogeri, G. Zodiatis, G. Kallos, 10-year high resolution study of wind, sea waves and wave energy assessment in the Greek offshore areas, Renew. Energy 90 (2016) 399–419.
[17] M.A. Hemer, S. Zieger, T. Durrant, J. O'Grady, R.K. Hoeke, K.L. McInnes, U. Rosebrock, A revised assessment of Australia's national wave energy resource, Renew. Energy 114 (2017) 85–107.
[18] Y. Lin, S. Dong, Z. Wang, C. Guedes Soares, Wave energy assessment in the China adjacent seas on the basis of a 20-year SWAN simulation with unstructured grids, Renew. Energy 136 (2019) 275–295.
[19] R. Carballo, N. Arean, M. Álvarez, I. López, A. Castro, M. López, G. Iglesias, Wave farm planning through high-resolution resource and performance characterization, Renew. Energy 135 (2019) 1097–1107.
[20] M. Vasileiou, E. Loukogeorgaki, D.G. Vagiona, GIS-based multi-criteria decision analysis for site selection of hybrid offshore wind and wave energy systems in Greece, Renew. Sustain. Energy Rev. 73 (2017) 745–757.
[21] Choong-Ki Kim, Jodie E. Toft, Michael Papenfus, Gregory Verutes, Anne D. Guerry, Marry H. Ruckelshaus, Katie K. Arkema, et al., Catching the right wave: evaluating wave energy resources and potential compatibility with existing marine and coastal uses, PLoS One 7 (No. 11) (2012) pe47598.
[22] L. Rusu, F. Onea, The performance of some state-of-the-art wave energy converters in locations with the worldwide highest wave power, Renew. Sustain. Energy Rev. 75 (2017) 1348–1362.
[23] L. Rusu, F. Onea, Assessment of the performances of various wave energy converters along the European continental coasts, Energy 82 (2015) 889–904.
[24] J. Morim, N. Cartwright, M. Hemer, A. Etemad-Shahidi, D. Strauss, Inter-and intra-annual variability of potential power production from wave energy converters, Energy 169 (2019) 1224–1241.
[25] B. Kamranzad, A. Etemad-Shahidi, V. Chegini, Developing an optimum hotspot identifier for wave energy extracting in the northern Persian Gulf, Renew. Energy 114 (2017) 59–71.
[26] S.G. Siegel, Numerical benchmarking study of a cycloidal wave energy converter, Renew. Energy 134 (2019) 390–405.
[27] P. Rosa-Santos, F. Taveira-Pinto, C.A. Rodríguez, V. Ramos, M. López, The CECO Wave Energy Converter: Recent Developments, Renewable Energy 139 (2019) 368–384.
[28] S. Diaconu, E. Rusu, The environmental impact of a Wave Dragon array operating in the Black Sea, Sci. World J. (2013) 1–20.
[29] A. Zanopol, F. Onea, E. Rusu, Coastal impact assessment of a generic wave farm operating in the Romanian nearshore, Energy 72 (No. 8) (2014) 652–670.
[30] A. Zanopol, F. Onea, E. Rusu, Evaluation of the coastal influence of a generic wave farm operating in the Romanian nearshore, J. Environ. Protect. Ecol. 15 (No. 2) (2014) 597–605.
[31] S. Contardo, R. Hoeke, M. Hemer, G. Symonds, K. McInnes, J. O'Grady, In situ observations and simulations of coastal wave field transformation by wave energy converters, Coast Eng. 140 (2018) 175–188.
[32] P. Balitsky, N. Quartier, G. Verao Fernandez, V. Stratigaki, P. Troch, Analyzing the near-field effects and the power production of an array of heaving cylindrical WECs and OSWECs using a coupled hydrodynamic-PTO model, Energies 11 (No. 12) (2018) 3489.
[33] C.E. Clark, A. Miller, B. DuPont, An analytical cost model for co-located floating wind-wave energy arrays, Renew. Energy 132 (2019) 885–897.
[34] F. Onea, E. Rusu, The expected efficiency and coastal impact of a hybrid energy farm operating in the Portuguese nearshore, Energy 97 (2016) 411–423.
[35] E. Rusu, F. Onea, S. Ciortan, E. Rusu, Assessment of the potential for development hybrid wind-wave projects in the European nearshore, Energy Environ. (2017) 1–18.
[36] F. Onea, L. Rusu, Coastal impact of a hybrid marine farm operating close to Sardinia Island, in: Proceedings of OCEANS'15 MTS/IEEE, Genova, May 18-21, 2015, pp. 1–7.
[37] A. Akpınar, B. Bingölbali, G. Ph Van Vledder, Wind and wave characteristics in the Black Sea based on the SWAN wave model forced with the CFSR winds, Ocean Eng. 126 (2016) 276–298.
[38] F. Onea, L. Rusu, A long-term assessment of the Black Sea wave climate, Sustainability 9 (No. 10) (2017) 1875.
[39] B.V. Divinsky, R.D. Kosyan, Spatiotemporal variability of the Black Sea wave climate in the last 37 years, Cont. Shelf Res. 136 (2017) 1–19.
[40] E. Rusu, A. Raileanu, A multi-parameter data-assimilation approach for wave prediction in coastal areas, J. Oper. Oceanogr. 9 (No. 1) (2016) 13–25.
[41] A. Raileanu, L. Rusu, E. Rusu, Data assimilation methods to improve the wave predictions in the Romanian coastal environment, in: Proceedings of SGEM2016, Informatics, Geoinformatics and Remote Sensing Conference, Albena, 30 June - 6 July, vol. II, 2016, pp. 855–862.
[42] L. Rusu, Wave modelling with data assimilation to evaluate the wave energy patterns in the Black Sea, in: Proceedings of 15th International Multidisciplinary Scientific GeoConference (SGEM2015)- Renewable Energy Sources and Clean Technologies, 16-25 June, Albena, vol. 4, 2015, pp. 597–606.
[43] D. Butunoiu, E. Rusu, Wave modeling with data assimilation to support the navigation in the Black Sea close to the Romanian ports, in: Proceedings of the Second International Conference on Traffic and Transport Engineering (ICTTE2014), Belgrad, November 27-28, 2014, pp. 180–187.
[44] E. Rusu, Wave Energy Assessments and Modeling of Wave-Current Interactions in the Black Sea, Macro-Engineering Seawater in Unique Environments: Arid Lowlands and Water Bodies Rehabilitation, 2011, pp. 213–259.
[45] L. Rusu, D. Ganea, E. Mereuta, A joint evaluation of wave and wind energy resources in the Black Sea based on 20-year hindcast information, Energy Explor. Exploit. 36 (No. 2) (2017) 335–351.
[46] Y. Saprykina, S. Kuznetsov, Analysis of the variability of wave energy due to climate changes on the example of the Black Sea, Energies 11 (No. 8) (2018) 2020.
[47] L. Rusu, Assessment of the wave energy in the Black Sea based on a 15-year hindcast with data assimilation, Energies 8 (No. 9) (2015) 10370–10388.
[48] N. Booij, R.C. Ris, L.H. Holthuijsen, A third generation wave model for coastal regions, Part 1: model description and validation, J. Geophys. Res. 104 (C4) (1999) 7649–7666.
[49] SWAN team, *Scientific and Technical Documentation*, SWAN Cycle III, Delft University of Technology, Department of Civil Engineering, the Netherlands, 2017.

[50] R.H. Moss, J.A. Edmonds, K.A. Hibbard, M.R. Manning, S.K. Rose, et al., The next generation of scenarios for climate change research and assessment, Nature 463 (No. 7282) (2010) 747–756.
[51] H. Holthuijsen, Waves in Oceanic and Coastal Waters, Cambridge University Press, 2010.
[52] E. Rusu, Strategies in using numerical wave models in ocean/coastal applications, J. Mar. Sci. Technol. Taiwan 19 (No. 1) (2011), 58-7.
[53] E. Rusu, Evaluation of the wave energy conversion efficiency in various coastal environments, Energies 7 (No. 6) (2014) 4002–4018.
[54] L. Rusu, M. Bernardino, C. Guedes Soares, Wind and wave modelling in the Black Sea, J. Oper. Oceanogr. 7 (No. 1) (2014) 5–20.
[55] L. Rusu, D. Butunoiu, Evaluation of the wind influence in modeling the Black Sea wave conditions, Environ. Eng. Manag. J. 13 (No. 2) (2014) 305–314.
[56] P.A.E.M. Janssen, Quasi-linear theory of wind-wave generation applied to wave forecasting, J. Phys. Oceanogr. 21 (1991) 1631–1642.
[57] E. Rusu, C.V. Soares, L. Rusu, Computational strategies and visualisation techniques for the wave modelling in the Portuguese nearshore, Marit. Transport. Exploit. Ocean Coast. Resour. 2 (2005) 1129–1136.
[58] L. Rusu, C. Guedes Soares, Impact of assimilating altimeter data on wave predictions in the western Iberian coast, Ocean Model. 96 (2015) 126–135.
[59] D.P. Van Vuuren, J. Edmonds, M. Kainuma, K. Riahi, A. Thomson, K. Hibbard, G.C. Hurtt, T. Kram, V. Krey, J.F. Lamarque, T. Masui, The representative concentration pathways: an overview, Clim. Change 109 (No. 1–2) (2011) 5.
[60] G. Strandberg, L. Bärring, U. Hansson, C. Jansson, C. Jones, E. Kjellström, M. Kolax, M. Kupiainen, G. Nikulin, P. Samuelsson, A. Ullerstig, S. Wang, *CORDEX Scenarios for Europe from the Rossby Centre Regional Climate Model RCA4*, Reports Meteorology and Climatology, No. 116, SMHI, Norrköping, Sweden, 2015. Available online at: https://www.smhi.se/polopoly_fs/1.90273!/Menu/general/extGroup/attachmentColHold/mainCol1/file/RMK_116.pdf.
[61] D. Jacob, J. Petersen, B. Eggert, A. Alias, O.B. Christensen, L.M. Bouwer, A. Braun, A. Colette, M. Déqué, G. Georgievski, E. Georgopoulou, A. Gobiet, L. Menut, G. Nikulin, A. Haensler, N. Hempelmann, C. Jones, K. Keuler, S. Kovats, N. Kröner, S. Kotlarski, A. Kriegsmann, E. Martin, E. van Meijgaard, C. Moseley, S. Pfeifer, S. Preuschmann, C. Radermacher, K. Radtke, D. Rechid, M. Rounsevell, P. Samuelsson, S. Somot, J.-F. Soussana, C. Teichmann, R. Valentini, R. Vautard, B. Weber, P. Yiou, EURO-CORDEX: new high-resolution climate change projections for European impact research, Reg. Environ. Change 14 (2014) 563–578.
[62] S. Kotlarski, K. Keuler, O.B. Christensen, A. Colette, M. Déqué, A. Gobiet, K. Goergen, D. Jacob, D. Lüthi, E. Van Meijgaard, G. Nikulin, C. Schär, C. Teichmann, R. Vautard, K. Warrach-Sagi, V. Wulfmeyer, Regional climate modeling on European scales: a joint standard evaluation of the EURO-CORDEX RCM ensemble, Geosci. Model Dev. 7 (No. 4) (2014) 1297–1333.
[63] E. Rusu, A 30-year projection of the future wind energy resources in the coastal environment of the Black Sea, Renew. Energy 139 (2019) 228–234.
[64] E. Kjellström, L. Bärring, G. Nikulin, C. Nilsson, G. Persson, G. Strandberg, Production and use of regional climate model projections - a Swedish perspective on building climate services, Clim. Serv. 2 (2016) 15–29.
[65] L. Rusu, A.B. Raileanu, F. Onea, A comparative analysis of the wind and wave climate in the Black Sea along the shipping routes, Water 10 (No. 7) (2018) 924.
[66] L. Mentaschi, M.I. Vousdoukas, E. Voukouvalas, A. Dosio, L. Feyen, Global changes of extreme coastal wave energy fluxes triggered by intensified teleconnection patterns, Geophys. Res. Lett. 44 (No. 5) (2017) 2416–2426.